

Structure, ferroelectric and piezoelectric properties of KNN-based perovskite ceramics

E. D. Politova, N. V. Golubko, G. M. Kaleva, A. V. Mosunov, N. V. Sadovskaya, S. Yu. Stefanovich, D. A. Kiselev, A. M. Kislyuk, M. V. Chichkov & P. K. Panda

To cite this article: E. D. Politova, N. V. Golubko, G. M. Kaleva, A. V. Mosunov, N. V. Sadovskaya, S. Yu. Stefanovich, D. A. Kiselev, A. M. Kislyuk, M. V. Chichkov & P. K. Panda (2019) Structure, ferroelectric and piezoelectric properties of KNN-based perovskite ceramics, *Ferroelectrics*, 538:1, 45-51, DOI: [10.1080/00150193.2019.1569984](https://doi.org/10.1080/00150193.2019.1569984)

To link to this article: <https://doi.org/10.1080/00150193.2019.1569984>



Published online: 17 May 2019.



Submit your article to this journal [↗](#)



View Crossmark data [↗](#)



Structure, ferroelectric and piezoelectric properties of KNN-based perovskite ceramics

E. D. Politova^a, N. V. Golubko^a, G. M. Kaleva^a, A. V. Mosunov^a, N. V. Sadovskaya^a, S. Yu. Stefanovich^a, D. A. Kiselev^{b,c}, A. M. Kislyuk^b, M. V. Chichkov^b, and P. K. Panda^d

^aL.Ya.Karpov Institute of Physical Chemistry, Moscow, Russia; ^bNational University of Science and Technology "MISIS", Moscow, Russia; ^cFryazino branch of the Koteln'nikov Institute of Radioengineering and Electronics of Russian Academy of Sciences, Fryazino, Russia; ^dNational Aerospace Laboratories, Kodihalli, Bangalore, India

ABSTRACT

Influence of donor (Ba) and acceptor (Ni) dopants on structure, microstructure, dielectric, ferroelectric and piezoelectric properties of $(K_{0.5}Na_{0.5})NbO_3$ ceramics have been studied. Dielectric parameters and effective d_{33} piezoelectric coefficients changes were observed depending on solid solutions compositions.

ARTICLE HISTORY

Received 14 May 2018
Accepted 31 October 2018


KEYWORDS

$(K_{0.5}Na_{0.5})NbO_3$; perovskite; ferroelectric; piezoelectric properties

1. Introduction

Potassium-sodium niobate $(K,Na)NbO_3$ (KNN) perovskite ceramics are being intensively studied as they are regarded among the most promising materials for replacement of piezoelectric materials containing toxic lead oxide [1–11]. It is known that piezoelectric properties of materials based on KNN are determined by the ratio of orthorhombic (O) and tetragonal (T) phases [8, 9, 12, 13]. Accordingly, to achieve larger piezoelectric response changes in KNN-based compositions are aimed to shift transition temperature from orthorhombic to tetragonal phase to the room temperature. And substitutions in A- and B-sites of perovskite lattice make most important contribution to changes in functional properties of piezoceramics. However, in spite of intensive research in studies of Pb-free compositions, development of lead-free family with properties comparable to those of lead zirconium-titanate (PZT) oxides is still a task to be solved. Main problems are related to difficulties in preparation of stoichiometric compositions and narrow sintering temperature interval for ceramics [13–21].

In this work, effects of modification of KNN compositions by donor (Ba^{2+}) and acceptor dopants (Ni^{3+}) in the A- and B-sites of perovskite lattice on structure, microstructure, dielectric, ferroelectric (FE) and piezoelectric properties of ceramics close to the Morphotropic Phase Boundary (MPB) in the $(1-x)(K_{0.5}Na_{0.5})NbO_3 - xBaTiO_3$ (KNN-BT) system ($x = 0.05$ and 0.06) additionally doped by the Ni^{3+} acceptor dopants in the $[(K_{0.5}Na_{0.5})_{1-x}Ba_x][(Nb_{1-x}Ti_x)_{1-y}Ni_y]O_3$ (KNN-BT-Ni) ($x = 0.05, 0.06; y = 0.01, 0.03, 0.05$) system have been studied.

CONTACT E. D. Politova  politova@nifhi.ru

Color versions of one or more of the figures in the article can be found online at www.tandfonline.com/gfer.

© 2019 Taylor & Francis Group, LLC

2. Experimental procedure

Ceramic samples in the KNN-BT-Ni system with $x=0.05, 0.06$; $y=0.01, 0.03, 0.05$; were prepared by the solid state reaction method at calcinations temperature $T_1 = 1073$ K (6 h), and sintering temperatures $T_2 = 1223$ and 1423 K (2 h). Sodium carbonate Na_2CO_3 , potassium carbonate K_2CO_3 , barium carbonate BaCO_3 , Nb_2O_5 , Ni_2O_3 and TiO_2 oxides (“pure” grade) were used as starting materials. Carbonates were dried at 673 K before synthesis in order to remove absorbed water.

Phase content and structure parameters of the samples were characterized by the X-ray Diffraction method (DRON-3M, Cu- K_α radiation with wavelength $\lambda = 1.5405$ Å, in the 2θ range of $5\text{--}80$ degrees). Raman measurements were performed with a RamMics M532 Raman microscope with spectral resolution of 5 cm^{-1} and estimated spot size of $2\text{ }\mu\text{m}$. Samples was excited using the 532 nm laser with an approximate 30 mW power output. The scattered radiation was detected by a 3648 pixel Linear CCD Array. All spectra were recorded at room temperature ($T = 298$ K), in the frequency region from 100 to 1400 cm^{-1} .

The Second Harmonic Generation (SHG) method was used to study spontaneous polarization and phase transitions of the samples (Nd:YAG laser, $\lambda = 1.064\text{ }\mu\text{m}$ in the reflection). Dielectric measurements were performed with fired silver electrodes on heating with 10 K/min . and cooling in the temperature interval of $300\text{--}1000$ K, in the frequency range of $100\text{ Hz--}1\text{ MHz}$ using Agilent 4284 A (1 V).

Microstructure of the samples was examined by the Scanning Electron Microscopy (SEM) method (JEOL YSM-7401F with JEOL JED-2300 energy dispersive X-ray spectrometer system).

Local piezoelectric hysteresis loops of the samples were characterized by piezoresponse force microscopy (PFM) method using a commercial scanning probe microscope MFP-3D (Asylum Research, USA) with Ti/Ir coated conductive probes (Asyelec-02, Asylum Research, USA). An AC voltage (3 V_{pp}) was superimposed onto a triangular square-stepping wave ($f = 0.5\text{ Hz}$ and bias window up to $\pm 50\text{ V}$) during the remnant piezoelectric hysteresis loops measurements.

3. Results and discussion

The samples with perovskite structure were prepared (Figure 1) though small amounts of admixture phase $\text{K}_2\text{Nb}_8\text{O}_{21}$ were observed in the X-ray diffraction patterns of the samples. The samples doped by the Ni^{3+} cations were characterized by pronounced texture with increased intensity of the $h00$ diffraction peaks (Figure 1, curves 3–7). These samples revealed tetragonal structure [21]. Slight decrease in the unit cell parameters observed due to introduction of small amount of Ni^{3+} -cations into B-sites positions of perovskite lattice was confirmed by changes in the A_1 (near $246\text{--}250\text{ cm}^{-1}$) and A_2 (near $601\text{--}606\text{ cm}^{-1}$) modes positions of Raman spectra [22] as well (Figure 2).

Microstructure of the samples is sensitive to composition and sintering conditions, and enlargement of mean size of grains was observed with increasing sintering temperature (Figure 3).

The SHG method confirmed that the samples belonged to the polar structures indicating to their FE. In the doped samples ferroelectric phase transitions were revealed by

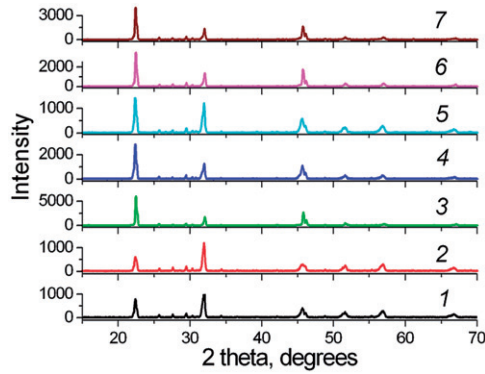


Figure 1. The X-ray diffraction patterns of the samples $(1-x)(\text{K}_{0.5}\text{Na}_{0.5})\text{NbO}_3-x\text{BaTiO}_3$ with $x = 0.05$ (1) and 0.06 (2), and of the samples $[(\text{K}_{0.5}\text{Na}_{0.5})_{1-x}\text{Ba}_x][(\text{Nb}_{1-x}\text{Ti}_x)_{1-y}\text{Ni}_y]\text{O}_3$ with $x = 0.05$, $y = 0.01$ (3), 0.03 (4), 0.05 (5) and with $x = 0.06$, $y = 0.01$ (6), 0.03 (7) prepared by the solid state reaction method at $T_1 = 1073\text{ K}$ (6 h), $T_2 = 1403\text{ K}$ (2 h).

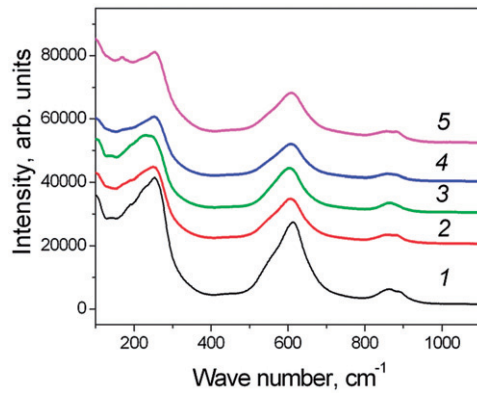


Figure 2. Raman spectra of $[(\text{K}_{0.5}\text{Na}_{0.5})_{1-x}\text{Ba}_x][(\text{Nb}_{1-x}\text{Ti}_x)_{1-y}\text{Ni}_y]\text{O}_3$ ceramics with $x = 0.05$, $y = 0$ (1), $y = 0.05$ (2), 0.01 (3), 0.03 (4), 0.05 (5) sintered at $T_2 = 1403\text{ K}$ (3–5) and at $T_2 = 1423\text{ K}$ (1, 2).

the SHG method. Increase in the spontaneous polarization value was observed in modified ceramics, and maximum intensity of the SHG signal $q = I_{2w}/I_{2w}(\text{SiO}_2) = 10000$ was revealed in the BaTiO_3 -doped samples KNN-BT with $x = 0.06$ sintered at $T_2 = 1413\text{ K}$ (2 h) [21].

Accordingly, ferroelectric phase transitions were revealed as steps at $T_{\text{pt}} \sim 400\text{ K}$ and as maxima at $T_{\text{m}} \sim 600\text{ K}$ in the dielectric permittivity versus temperature curves (Figure 4). Slight decrease in temperatures of both phase transitions was observed in ceramic solid solutions with increasing Ni^{3+} content. At the room temperature, non monotonous changes of dielectric parameters and spontaneous polarization values were observed in modified compositions studied.

Using the PFM method the as-grown domain structure was observed in ceramics prepared. Simultaneous topography and out-of-plane PFM images showed that the imaged pattern were due to the piezoresponse of the patterns [21]. Complex domain structure consisting of multiple domain patterns was found for investigated ceramics. Two points on the surface of ceramics were chosen to measure the local piezoresponse at selected

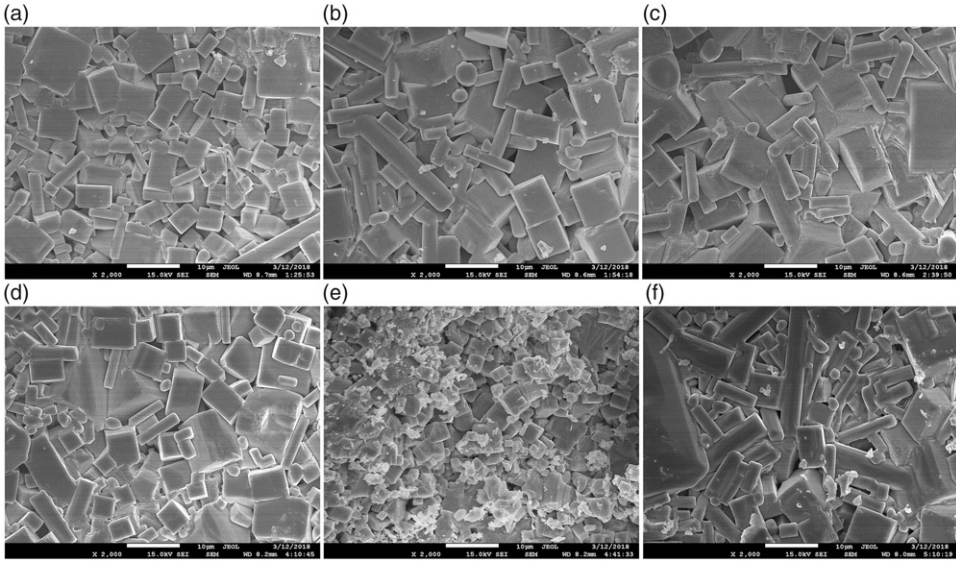


Figure 3. Microstructure of the surface of the $[(K_{0.5}Na_{0.5})_{1-x}Ba_x][(Nb_{1-x}Ti_x)_{1-y}Ni_y]O_3$ samples with $x = 0.05$, $y = 0.01$ (a), 0.03 (b), 0.05 (c), with $x = 0.06$, $y = 0.01$ (d), 0.03 (e), 0.05 (f) sintered at $T_2 = 1403$ K (2 h). Bars – $10 \mu\text{m}$.

regions. The first regions were located at the area with large domain contrast while the second regions were areas with weak piezoresponse signal in the PFM images [21]. The hysteresis behavior of the piezoresponse confirmed FE switching of the ceramic (Figure 5). Effective d_{33} piezoelectric coefficient values reached $d_{33} = 280$ pm/V in the KNN-BT ceramics, while effective d_{33} values for KNN-BT-Ni ceramics with $x = 0.05$ measured at $V_{DC} = 50$ V decreased from $d_{33} = 273$ ($x = 0.05$, $y = 0.00$) to 163 pm/V ($x = 0.05$, $y = 0.05$).

The loops measured on region with large PFM contrast are shifted towards either to positive or negative bias voltage. This effect indicates to the presence of internal bias fields stabilizing energetically favorable orientation of the polarization along their directions, and resulting in an asymmetry of the switching process [23, 24]. Moreover, the values of effective d_{33} measured at $+50$ V are lower than those recorded at -50 V for KNN-BT-Ni ceramics with $x = 0.05$ and $y = 0, 0.01, 0.05$. Such effects may be explained by the presence of non- 180° domains in ceramics [25]. As shown in Figure 5, effective d_{33} piezoelectric coefficient values reached 280 pm/V in the KNN-BT samples and 160 pm/V in the KNN-BT samples doped by the Ni^{3+} cations measured for $+50$ V; and minimum values -400 pm/V and -240 pm/V measured at -50 V for KNN-BT and KNN-BT-Ni samples, respectively. Such behavior is consistent with known effect that domain walls motion is hindered in the acceptor doped materials due to a large energy difference among different positions of an oxygen vacancy in the oxygen octahedra of the perovskite unit cell [26]. These PFM results correlate well with concentration dependence of dielectric permittivity values measured at the room temperature. The results obtained confirmed prospects of new lead-free materials development by modification of the KNN-based compositions close to the MPB by the aliovalent cation substitutions.

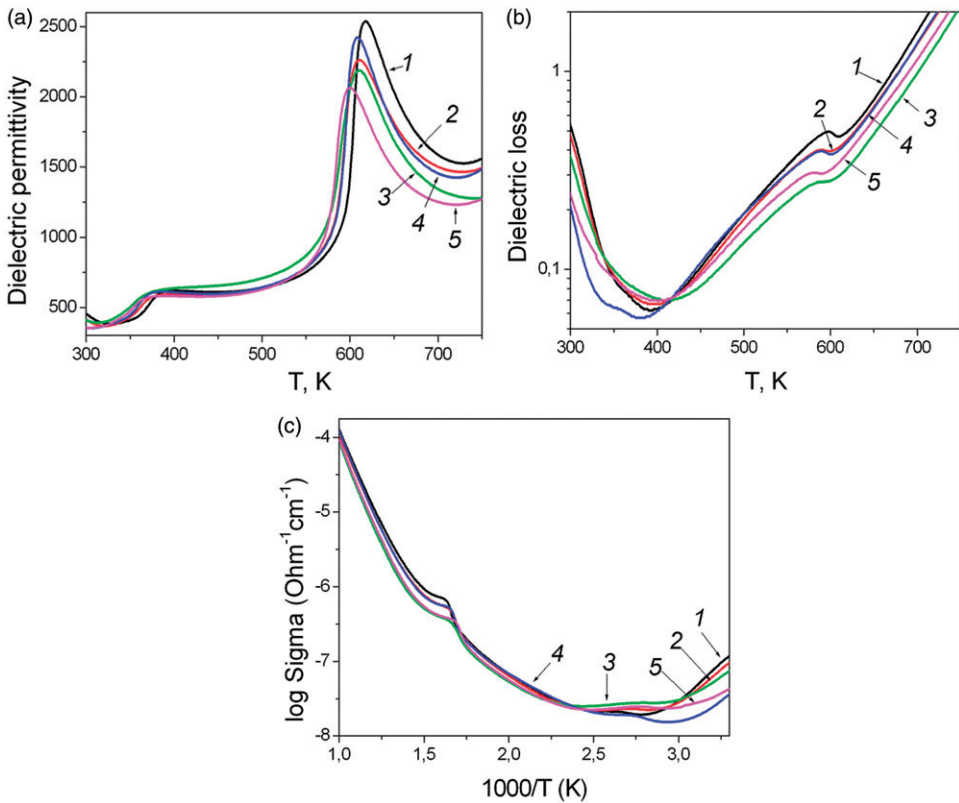


Figure 4. Temperature dependences of dielectric permittivity $\varepsilon(T)$, dielectric loss $\tan\delta(T)$ and electro-conductivity $\log \text{Sigma}$ ($1/T$) of the samples $[(\text{K}_{0.5}\text{Na}_{0.5})_{1-x}\text{Ba}_x][(\text{Nb}_{1-x}\text{Ti}_x)_{1-y}\text{Ni}_y]\text{O}_3$ with $x = 0.05$ (1, 2) and 0.06 (3, 4), $y = 0.01$ (1, 3), 0.03 (2, 4), 0.05 (5) sintered at $T_3 = 1403$ K (2h) measured at frequency $f = 1$ kHz.

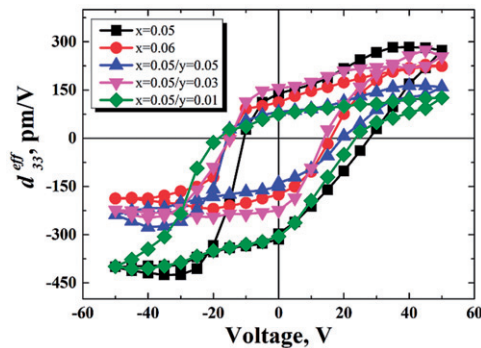


Figure 5. Local PFM hysteresis loops from regions showed larger domain contrast in the VPFM images.

4. Conclusions

Structure parameters, microstructure, dielectric, ferroelectric and piezoelectric properties of ceramics in the $[(\text{K}_{0.5}\text{Na}_{0.5})_{1-x}\text{Ba}_x][(\text{Nb}_{1-x}\text{Ti}_x)_{1-y}\text{Ni}_y]\text{O}_3$ system were studied. Slight changes in the unit cell volume and temperatures of phase transitions were observed

depending on composition and sintering conditions. High values of dielectric parameters and effective d_{33} piezoelectric coefficients were observed thus confirming prospects of the KNN-based ceramics for development of new efficient materials.

Disclosure statement

No potential conflict of interest was reported by the authors.

Funding

The work was supported by the Russian Foundation for Basic Research (Project 16-53-48009). PFM studies were performed at Center for Shared Use “Material Science and Metallurgy” at the National University of Science and Technology “MISiS” and were supported by the Ministry of Education and Science of the Russian Federation (project n 11.9706.2017/7.8).

References

- [1] S. J. Zhang, R. Xia, and R. T. Shroud, Lead-free piezoelectric ceramics: Alternatives for PZT? *J Electroceram.* **19**(4), 251 (2007).
- [2] T. Takenaka, H. Nagata, and Y. Hiruma, Current developments and prospective of lead-free piezoelectric ceramics, *Jpn. J. Appl. Phys.* **47**(5), 3787 (2008). DOI: [10.1143/JJAP.47.3787](https://doi.org/10.1143/JJAP.47.3787).
- [3] P. K. Panda, Review: Environmental friendly lead-free piezoelectric materials, *J. Mater. Sci.* **44**(19), 5049 (2009). DOI: [10.1007/s10853-009-3643-0](https://doi.org/10.1007/s10853-009-3643-0).
- [4] D. DAMJANOVIC, N. KLEIN, J. LI, and V. POROKHONSKYY, What can be expected from lead-free piezoelectric materials? *Funct. Mater. Lett.* **03**(01), 5 (2010). DOI: [10.1142/S1793604710000919](https://doi.org/10.1142/S1793604710000919).
- [5] D. Q. Xiao, Progresses and further considerations on the research of perovskite lead-free piezoelectric ceramics, *J. Adv. Dielect.* **01**(01), 33 (2011). DOI: [10.1142/S2010135X11000045](https://doi.org/10.1142/S2010135X11000045).
- [6] Y. Q. Lu, and Y. X. Li, A review on lead-free piezoelectric ceramics studied in China, *J. Adv. Dielect.* **01**(03), 269 (2011). DOI: [10.1142/S2010135X11000409](https://doi.org/10.1142/S2010135X11000409).
- [7] I. Coondoo, N. Panwar, and A. Kholkin, Lead-free piezoelectrics: Current status and perspectives. *J. Adv. Dielect.* **03**(02), 1330002 (2013). DOI: [10.1142/S2010135X13300028](https://doi.org/10.1142/S2010135X13300028).
- [8] J. F. Li *et al.*, (K, Na)NbO₃-based lead-free piezoceramics: Fundamental aspects, processing technologies, and remaining challenges. *J. Am. Ceram. Soc.* **96**(12), 3677 (2013). DOI: [10.1111/jace.12715](https://doi.org/10.1111/jace.12715).
- [9] J. G. Wu, D. Q. Xiao, and J. G. Zhu, Potassium-sodium niobate lead-free piezoelectric materials: Past, present, and future of phase boundaries. *Chem. Rev.* **115**(7), 2559 (2015). DOI: [10.1021/cr5006809](https://doi.org/10.1021/cr5006809).
- [10] P. K. Panda, and B. Sahoo, PZT to lead-free piezo ceramics. *Ferroelectrics* **474**(1), 128 (2015). DOI: [10.1080/00150193.2015.997146](https://doi.org/10.1080/00150193.2015.997146).
- [11] C. H. Hong *et al.*, J. Lead-free piezoceramics. Where to move on? *J. Materiomics* **2**(1), 1 (2016). DOI: [10.1016/j.jmat.2015.12.002](https://doi.org/10.1016/j.jmat.2015.12.002).
- [12] Y. J. Dai, X. W. Zhang, and K. P. Chen, Morphotropic phase boundary and electrical properties of K_{1-x}NaxNbO₃ lead-free ceramics, *Appl. Phys. Lett.* **94**(4), 042905 (2009). DOI: [10.1063/1.3076105](https://doi.org/10.1063/1.3076105).
- [13] K. Wang, and J. F. Li, (K,Na)NbO₃-based lead-free piezoceramics: Phase transition, sintering and property enhancement. *J. Adv. Ceram.* **1**(1), 24 (2012). DOI: [10.1007/s40145-012-0003-3](https://doi.org/10.1007/s40145-012-0003-3).

- [14] H.-Y. Park *et al.*, Microstructure and piezoelectric properties of $0.95(\text{Na}_{0.5}\text{K}_{0.5})\text{NbO}_3\text{-}0.05\text{BaTiO}_3$ ceramics, *Appl. Phys. Lett.* **89**(6), 062906 (2006). DOI: [10.1063/1.2335816](https://doi.org/10.1063/1.2335816).
- [15] J. Fang *et al.*, Narrow sintering temperature window for (K,Na) NbO_3 -based lead-free piezoceramics caused by compositional segregation. *Phys. Status Solidi A.* **208**(4), 791 (2011).
- [16] R. Zuo *et al.*, Sintering and electrical properties of lead-free $\text{Na}_{0.5}\text{K}_{0.5}\text{NbO}_3$ piezoelectric ceramics. *J. Am. Ceramic Soc.* **89**(6), 2010 (2006).
- [17] S. Zhang, R. Xia, and T. R. Shrout, Modified $(\text{K}_{0.5}\text{Na}_{0.5})\text{NbO}_3$ based lead-free piezoelectrics with broad temperature usage range. *Appl. Phys. Lett.* **91**(13), 132913 (2007). DOI: [10.1063/1.2794400](https://doi.org/10.1063/1.2794400).
- [18] J. Tellier *et al.*, Crystal structure and phase transitions of sodium potassium niobate perovskites. *Solid State Sci.* **11**(2), 320 (2009). DOI: [10.1016/j.solidstatesciences.2008.07.011](https://doi.org/10.1016/j.solidstatesciences.2008.07.011).
- [19] B. Malič *et al.*, Sintering of lead-free piezoelectric sodium potassium niobate ceramics. *Materials.* **12**, 8117 (2015). DOI: [10.3390/ma8125449](https://doi.org/10.3390/ma8125449).
- [20] E. D. Politova *et al.*, Influence of NaCl/LiF additives on structure, microstructure and phase transitions of $(\text{K}_{0.5}\text{Na}_{0.5})\text{NbO}_3$ ceramics. *Ferroelectrics.* **489**(1), 147 (2015). DOI: [10.1080/00150193.2015.1070248](https://doi.org/10.1080/00150193.2015.1070248).
- [21] E. D. Politova *et al.*, Processing and characterization of lead-free ceramics on the base of sodium-potassium niobate. *J. Adv. Dielect.* **08**(01), 1850004 (2018). DOI: [10.1142/S2010135X18500042](https://doi.org/10.1142/S2010135X18500042).
- [22] M. A. M. Harttar, M. W. A. Rashid, and U. A. A. Azlan, Physical and electrical properties enhancement of rare-earth doped potassium-sodium niobate (KNN): A review. *Ceramics - Silikaty.* **59**, 158 (2015).
- [23] S. Jesse, A. P. Baddorf, and S. V. Kalinin, Switching spectroscopy piezoresponse force microscopy of ferroelectric materials. *Appl. Phys. Lett.* **88**(6), 062908 (2006). DOI: [10.1063/1.2172216](https://doi.org/10.1063/1.2172216).
- [24] H. Trivedi *et al.*, Local manifestations of a static magnetoelectric effect in nanostructured $\text{BaTiO}_3\text{-BaFe}_{12}\text{O}_{19}$ composite multiferroics. *Nanoscale* **7**(10), 4489 (2015). DOI: [10.1039/C4NR05657D](https://doi.org/10.1039/C4NR05657D).
- [25] D. E. Dausch, Asymmetric 90° domain switching in rainbow actuators. *Ferroelectrics* **210**(1), 31 (1998). DOI: [10.1080/00150199808229911](https://doi.org/10.1080/00150199808229911).
- [26] T. Rojac, and D. Damjanovic, Domain walls and defects in ferroelectric materials. *Jpn. J. Appl. Phys.* **56**(10S), 10PA01 (2017). DOI: [10.7567/JJAP.56.10PA01](https://doi.org/10.7567/JJAP.56.10PA01).